SSRG International Journal of Electrical and Electronics Engineering
ISSN: 2348-8379/ https://doi.org/10.14445/23488379/IJEEE-V13I9P107

Volume 13 Issue 9, 85-92, September 2026

Original Article

Integrated Design of a 2.45 GHz Phased Array Antenna with MEMS-based DMTL Phase Shifters

Mohd Saiful Riza Bashri[1], Noor Amalina Ramli[2], Nur Afifah Athirah Khairul Bahari[3]

[1]Department of Science, Kulliyyah of Engineering, International Islamic University Malaysia, Malaysia.
[2]Department of Electrical and Electronic Engineering, Universiti Pertahanan Nasional Malaysia, Malaysia.

[2]Corresponding Author : nooramalina@upnm.edu.my

Received: 12 February 2026 Revised: 28 April 2026 Accepted: 05 September 2026 Published: 26 September 2026

Abstract *- This work presents a system-level study of a 2.45 GHz phased array antenna that incorporates MEMS-based Distributed MEMS Transmission Line (DMTL) phase shifters. The RF front-end is formed by combining a cascaded 2-bit DMTL phase-shifting section, a four-way Wilkinson divider, and a four-element microstrip patch array. Each RF section was initially designed and refined separately using full-wave electromagnetic simulation before being connected in ANSYS AEDT to assess the complete system response. The beam-steering behaviour was studied by varying the phase excitation introduced by the DMTL phase-shifting network. The simulated array steered the main beam from -20° to +20° and achieved a maximum gain of 10.56 dBi. Electrothermal analysis was also included to estimate the temperature distribution of the antenna structure under 30 mW input power. The results indicate that the proposed integrated configuration provides practical beam steering performance with acceptable RF matching and thermal behaviour for compact reconfigurable wireless systems.*

Keywords *- Phased array antenna, DMTL phase shifter, RF MEMS, Beam steering, Wilkinson power divider.*

1. Introduction

The rapid growth of wireless communication has increased the need for antenna systems that can direct radiated energy more efficiently. Phased arrays are suitable for this application because their radiation direction can be adjusted electronically through phase control between the radiating elements. This capability is useful for applications that require directional coverage, adaptive links, and compact antenna platforms. For such systems, the phase-shifting network must provide accurate phase control while keeping insertion loss, size, and power consumption low.

As shown conceptually in Figure 1, beam steering in a phased array is achieved by applying a controlled progressive phase difference between adjacent antenna elements. This method enables beam redirection without requiring mechanical movement of the antenna structure.

The steering range, gain, and matching performance depend on several design factors, including array size, element separation, feed configuration, and phase-shifter characteristics. Therefore, the phase shifter must be designed together with the antenna and feed network rather than being treated only as a separate device [2, 3].

Microwave phase control has been implemented using several technologies, such as PIN diode circuits, CMOS-based circuits, switched-line networks, and RF MEMS structures [3-6]. PIN diode and CMOS phase shifters are useful in many integrated RF circuits, but their performance can be affected by insertion loss, power consumption, bandwidth, and linearity limitations.

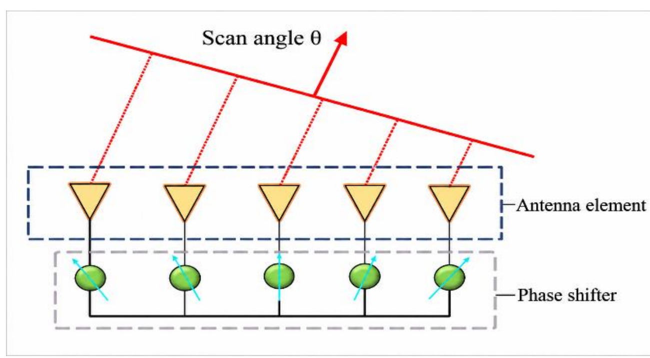

Fig. 1 Phase array antenna

RF MEMS technology offers another route because it can provide low RF loss, high isolation, and good linearity in a compact structure [7-9]. Two common MEMS phase-shifter topologies are the switched-line phase shifter and the Distributed MEMS Transmission Line (DMTL) phase shifter. In a DMTL structure, MEMS capacitive loading is distributed along the transmission line, allowing the signal phase velocity to be modified.

When the MEMS bridges are actuated, the effective capacitance along the transmission line changes. This changes the line impedance and propagation velocity, which produces the required differential phase delay. Since the delay is distributed along the line, the DMTL topology is suitable for broadband phase-control applications. This feature is important in array systems because phase-shifter behaviour can affect beam squint, particularly when the operating bandwidth is large [10]. Previous studies have mainly focused on component-level DMTL phase shifters and RF-MEMS switching structures rather than complete phased-array antenna integration [7-9, 11]. In comparison, fewer studies have investigated the system-level integration of MEMS-based DMTL phase shifters with the feeding network and antenna array, particularly at 2.45 GHz. In addition, many reported studies analyse the antenna, phase shifter, and feeding network separately, so the interaction between the RF blocks is not fully captured at system level. This motivates an integrated simulation workflow that combines the DMTL phase shifter, power divider, antenna array, beam steering analysis, and thermal assessment in one design environment.

This paper presents an integrated 2.45 GHz phased array antenna developed using ANSYS Electronics Desktop (AEDT). The system combines a 2-bit cascaded DMTL phase shifter, a 4-way Wilkinson power divider, and a 4-element microstrip patch array. The DMTL phase shifter uses 16 shunt MEMS switches loaded on a Coplanar Waveguide (CPW) transmission line to obtain the required 0º and 90º phase states at the target frequency. Each RF block was first simulated in ANSYS HFSS to verify its return loss, insertion loss, phase response, and antenna characteristics. The verified component models were then connected in ANSYS Nexxim to evaluate the beam steering response of the complete RF system. Finally, the electromagnetic loss was coupled to ANSYS Icepak to estimate the temperature rise of the antenna array under the selected input power.

The main contribution of this work is the demonstration of a co-simulated RF system at 2.45 GHz that links electromagnetic, circuit-level, and thermal analyses for a MEMS-based phased array antenna. This gives a more realistic evaluation of the integrated system compared with evaluating the phase shifter, power divider, and antenna array independently.

2. Literature Review

Phase shifters are central to phased array antennas because they determine the phase progression between radiating elements. By changing this phase progression, the main radiation beam can be moved without changing the physical position of the antenna. Several technologies have been used for this function, including PIN diode, CMOS, and MEMS-based phase shifters [3]. PIN diode designs generally provide fast switching, but they may introduce additional RF loss and limited linearity at some operating conditions. CMOS phase shifters are compatible with integrated circuit processes, although their RF performance and power consumption may become limiting factors. RF MEMS phase shifters are attractive because they can offer low insertion loss, high isolation, and high linearity.

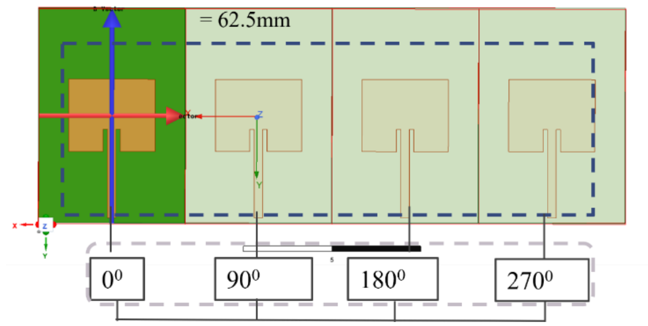

Fig. 2 Element patch array antenna with phase shifter

Among MEMS-based configurations, the DMTL phase shifter is a promising structure for controllable delay and phase variation [9, 11]. It is formed by placing MEMS capacitive bridges periodically along a high-impedance transmission line. The state of the MEMS bridges changes the distributed capacitance of the line and consequently modifies the phase velocity of the RF signal. Earlier studies have shown that DMTL phase shifters can achieve useful phase accuracy and low loss at microwave frequencies. However, these studies have primarily focused on component-level phase-shifter performance rather than integration with complete phased-array antenna systems.

Wilkinson dividers are widely used in array feeding networks because they can distribute power to multiple ports while maintaining matching and port isolation. Wilkinson power dividers have also been successfully integrated with microstrip antenna arrays in previous RF systems to provide controlled power distribution among multiple antenna elements**.** However, many phased array studies still report the antenna array, phase-shifter network, and feed network as separate designs.

This study addresses the above gap by integrating a MEMS-based DMTL phase shifter, a 4-way Wilkinson divider, and a 4-element microstrip patch antenna array in a single 2.45 GHz phased array system. Thermal analysis is also included so that the effect of electromagnetic loss on the antenna temperature can be observed.

3. Design and Simulation Workflow

The design process followed a two-stage simulation procedure. First, the DMTL phase shifter, Wilkinson power divider, and 4-element patch array were designed and optimized separately in ANSYS HFSS. The main parameters checked at this stage were return loss, insertion loss, phase shift, gain, and impedance matching. After each block achieved acceptable RF performance, the components were connected in ANSYS Nexxim for system-level co-simulation.

In this integrated model, the input phase conditions were varied to observe the beam steering response. The electromagnetic loss from HFSS was then used in ANSYS Icepak to calculate the temperature distribution of the antenna array.

3.1. DMTL Phase Shifter

The DMTL phase shifter in this work is modelled as a two-port RF network that introduces a controlled phase delay to the signal travelling along the line. The phase shifter is based on a CPW line with periodically placed MEMS shunt bridge elements, as shown in Figure 4.

The effective line capacitance is determined by the actuation state of the MEMS bridges. In the up-state, the capacitive loading is lower and the signal travels with a smaller delay. In the down-state, the added capacitance increases the delay and produces the required phase shift. The switch capacitance is estimated using the parallel-plate relation in Equation (1) [12].

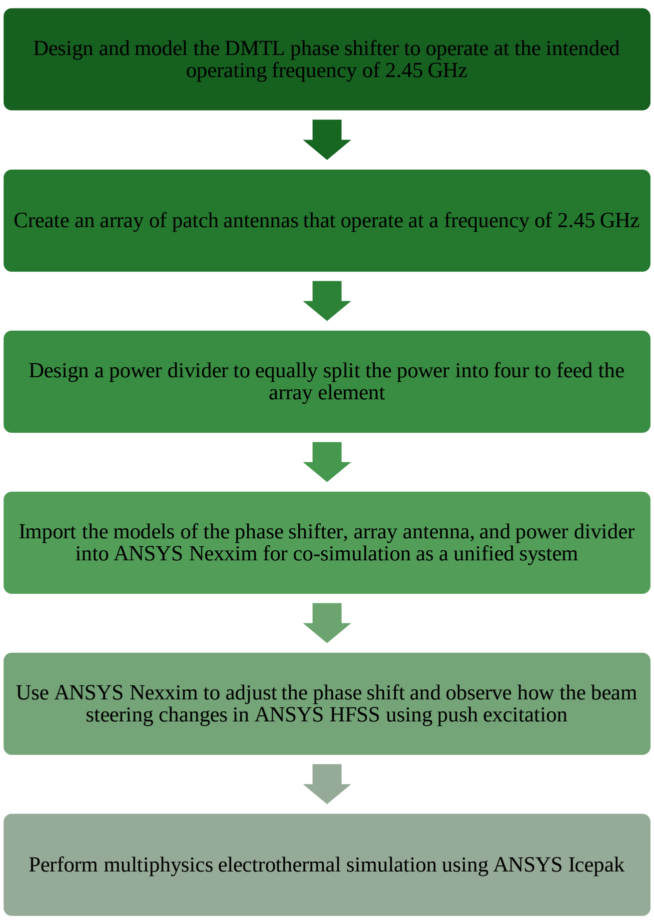

Fig. 3 Simulation flow

$$C_{pp} = \frac{\varepsilon_o A}{g_o + \frac{t_d}{\varepsilon_r}} \quad (1)$$

Where ε_0 is the permittivity of free space, A is the overlap area of the bridge and transmission line, g_0 is the initial air gap, t_d is the dielectric thickness, and ε_r is the dielectric constant of the dielectric layer.

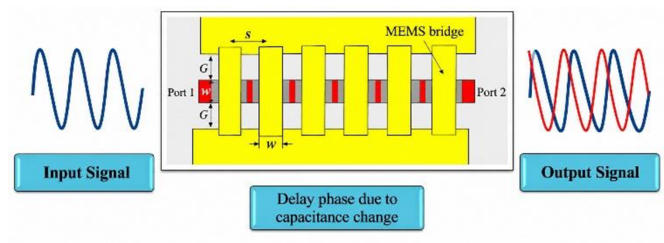

Fig. 4 Working principle of DMTL phase shifter

The complete DMTL phase shifter structure used in this study is shown in Figure 5. 16-unit cells were selected to realize the required phase response, corresponding to 0º in the up-state and 90º in the down-state at approximately 2.45 GHz. The spacing between adjacent MEMS bridges was set to 1850 µm and was determined using Equation (2) [12].

$$S = \frac{Z_d c}{\pi f_b Z_o \sqrt{\varepsilon_{r,eff}}} \quad (2)$$

where Z_d is the down-state distributed impedance of the DMTL, Z_0 is the characteristic impedance of the unloaded line, c is the speed of light, ε_{eff} is the effective dielectric constant of the unloaded line, and f_B is the Bragg frequency, as expressed in Equation (3) [12].

$$f_B = \frac{2}{2\pi\sqrt{sSL_t(sC_t + C_b)}} \quad (3)$$

In this design, the Bragg frequency was selected to be ten times higher than the 2.45 GHz operating frequency. This selection keeps the operating band sufficiently below the periodic-line cutoff region and helps avoid a strongly reflective response when the MEMS bridges are in the down-state.

The phase shifter was implemented on a high-resistivity silicon substrate with a thickness of 525 µm and a resistivity of 10 kOhm.cm. This substrate was selected to reduce RF losses through the supporting material.

The loaded impedances were set to 60 Ohm for the up-state and 42 Ohm for the down-state to obtain acceptable matching for the different phase states. The main geometrical and electrical parameters of the DMTL phase shifter are listed in Table 1. The RF response of the phase shifter was evaluated in ANSYS HFSS.

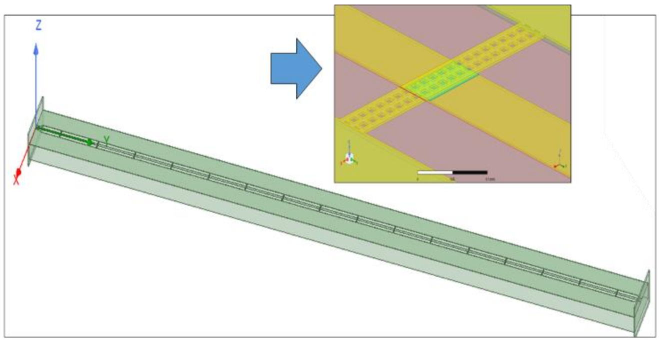

Fig. 5 DMTL phase shifter structure

Table 1. DMTL phase shifter parameters

Parameters	Value
Z_0	65Ω
Z_u	60Ω
Z_d	42Ω
CPW (G/W/G)	136/100/136 µm
Thickness of CPW	2 µm
Distance between beam, s	1850 µm
Beam dimension (w x L)	50 × 372 µm
Thickness of beam	1 µm
Air gap	1.5 µm
Bragg freq, f_{Bragg}	10 f_0
Upstate capacitance, C_{lu}	45.38fF
Downstate capacitance, C_{ld}	363.014fF
Capacitance ratio, C_r	8
Cells	16

3.2. Microstrip Antenna Array

A rectangular patch element operating around 2.45 GHz was modelled and optimized in ANSYS HFSS. Radiation from the patch mainly occurs due to fringing fields along its edges, while its resonant frequency is strongly related to the effective patch length. For the dominant TM10 mode, the approximate resonant frequency can be calculated using Equation (4) [12].

$$f_o = \frac{c}{2L\sqrt{\varepsilon_{eff}}} \quad (4)$$

Where c is the speed of light, L is the effective patch length, and ε_{eff} is the effective dielectric constant. The single-element antenna dimensions are summarized in Table 2. After the unit element was optimized, four identical elements were arranged to form the antenna array. The finite array was simulated using the Finite Array Domain Decomposition Method (FADDM), which reduces computational cost while still accounting for coupling between elements. Figure 6 shows a single unit patch antenna at 2.45GHz modelled in Ansys HFSS.

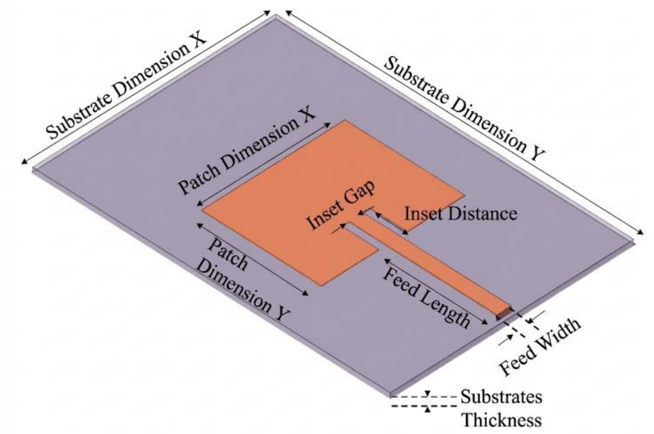

Fig. 1 Single unit patch antenna at 2.45 GHz

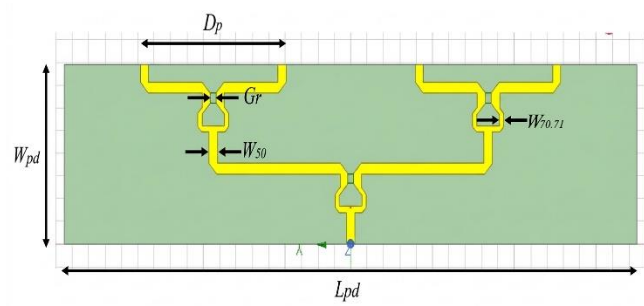

Fig. 7 4-way Wilkinson power divider

Table 2. 2.45 GHz patch antenna parameter

Parameters	**Value (cm)**
Frequency	2.45 GHz
Patch Dimension X	1.19
Patch Dimension Y	0.91
Substrate Material	FR-4
Substrate Dimension X	2.7
Substrate Dimension Y	2.87
Substrate Thickness	0.1575
Feed Width	0.493
Feed Length	0.914
Inset Distance	0.276
Inset Gap	0.247

3.3. Wilkinson Power Divider

The feed network used a four-way Wilkinson divider to distribute the input signal into four matched branches. The divider was designed for a 50 Ohm system and optimized so that the output spacing matched the physical spacing of the antenna array. This reduces the need for additional interconnect transitions during system integration. The final divider layout is shown in Figure 7, and its optimized dimensions are given in Table 3.

3.4. Co-Simulation

The complete phased array was analysed using co-simulation in ANSYS AEDT. The validated HFSS component models were brought into ANSYS Nexxim and interconnected to form the complete RF network. This approach allows the circuit-level signal distribution and the electromagnetic response of the antenna to be evaluated together. In the Nexxim environment, each HFSS component is represented by its corresponding port-based model.

The Wilkinson divider splits the input power into four signal paths, while the cascaded DMTL phase shifters introduce the required phase states before the signals are applied to the antenna elements.

Table 3. Geometrical parameter of the 4-way wilkinson power divider

Parameters	Value
Length, *Lpd*	350mm
Width, *Wpd*	79mm
Port separation distance, *Dp*	84mm
Feedline width for 50Ω TL, *W50*	4.93mm
Feedline width for 70.71Ω TL, *W70.71*	2.78mm
Branches gap, *Gr*	3.42mm
Resistor 1	100Ω
Resistor 2	100Ω
Resistor 3	100Ω

By changing the phase progression between the four elements, the main beam direction can be adjusted. In this work, three DMTL phase-shifter units were connected in series in the required paths to realize phase states of 0º, 90º, 180º, and 270º for the array excitation.

3.5. Thermal Analysis

ANSYS Icepak was used to evaluate the temperature profile of the four-element patch array. The electromagnetic loss calculated in HFSS was transferred to Icepak and treated as the heat source. This electrothermal coupling is useful because RF losses in the metal and substrate can create localized heating, especially when the antenna is operated continuously.

For the thermal setup, the antenna array was first solved in HFSS with an input power of 30 mW. The model was then transferred to Icepak for steady-state thermal analysis. Opening boundaries were applied at the inlet and outlet regions, while the substrate, antenna metallization, and ground plane were assigned as EM-loss regions, as shown in Figure 9.

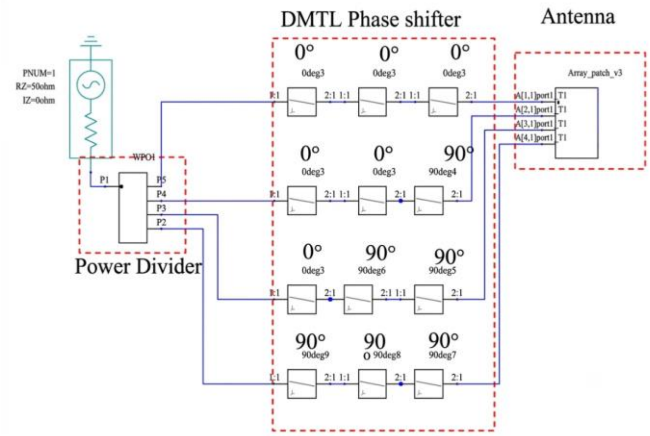

Fig. 8 Co-simulation in ANSYS Nexxim

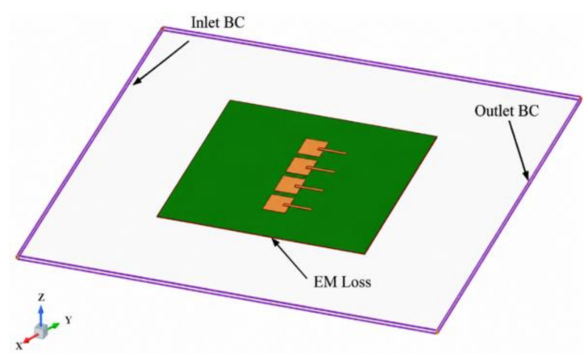

Fig. 9 Thermal boundary condition in ANSYS icepak

4. Results and Discussion

4.1. DMTL Phase Shifter

The DMTL phase shifter performance was evaluated based on its matching, transmission loss, and phase response. As shown in Figure 10, both up-state and down-state cases-maintained return loss below -10 dB over the 2 GHz to 4 GHz range, indicating acceptable impedance matching. This response was obtained using loaded impedances of 60 Ohm in the up-state and 42 Ohm in the down-state. At 2.45 GHz, the simulated insertion losses were -0.68 dB and -0.86 dB for the 0º and 90º states, respectively, as shown in Figure 11. The corresponding phase response is presented in Figure12.

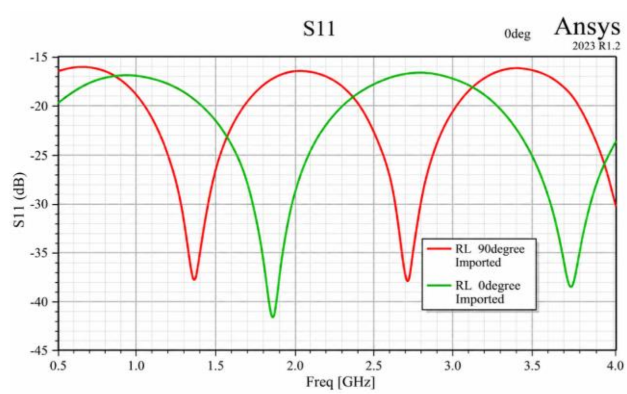

Fig. 10 Return loss of phase shifter10

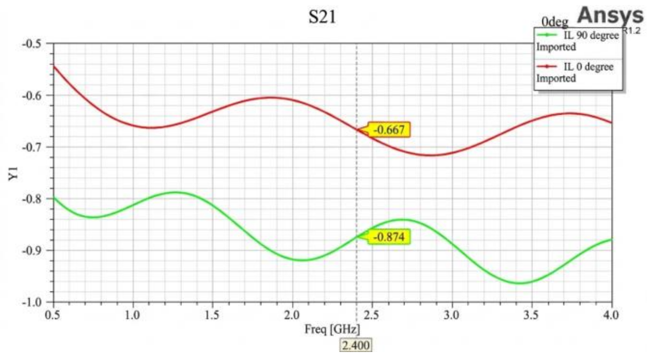

Fig. 11 Insertion loss of DMTL phase shifter

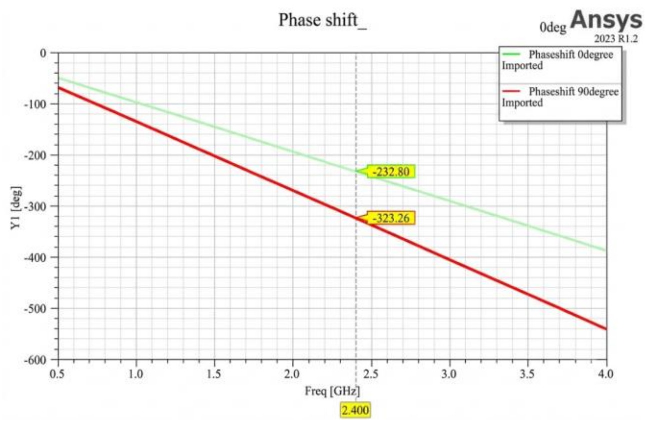

Fig. 12 Phase shift of DMTL phase shifter

4.2. Patch Array Antenna

At approximately 2.45 GHz, the simulated array achieved a reflection coefficient of -15.84 dB, confirming that the array was reasonably matched. The radiation pattern in Figure 14 shows a directional response with a simulated gain of 10.56 dBi. These results indicate that the 4-element patch array is suitable for integration with the phase-shifting and power-dividing network.

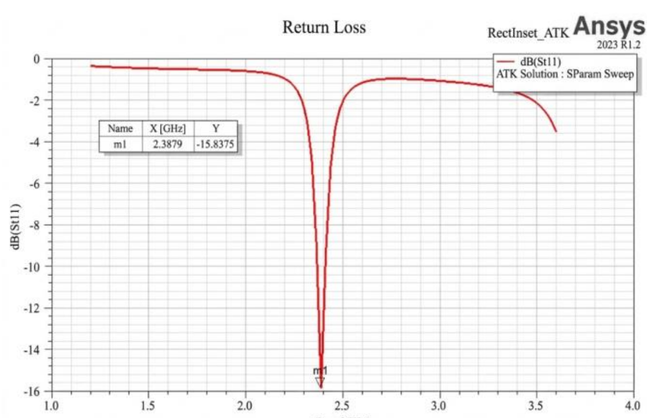

Fig. 13 Reflection coefficient of the patch array antenna

4.3. Wilkinson Power Divider

The simulated S-parameter response of the 4-way Wilkinson power divider is shown in Figure 15. The input and output ports remained below -10 dB around the operating frequency, showing good impedance matching. The transmission coefficient from the input port to the four output ports was approximately -6.35 dB to -6.37 dB, which is close to the theoretical 4-way power division level with a small additional insertion loss of about 0.36 dB.

4.4. Co-Simulation

The integrated phased array was evaluated by observing the beam direction under different progressive phase excitations. After the power divider, the DMTL phase shifters provided the required phase conditions to the antenna elements.

The simulated radiation patterns show that the main beam can be steered to approximately -20º and +20º. The return loss values for the three beam directions are summarized in Table 4. Increasing the number of antenna elements or increasing the phase-shifter resolution would allow finer beam steering control.

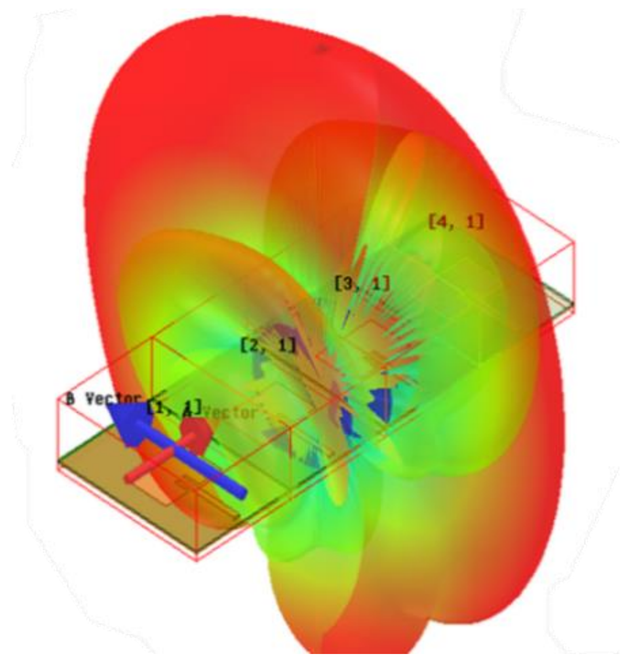

Fig. 14 Radiation pattern of 4-element patch array antenna

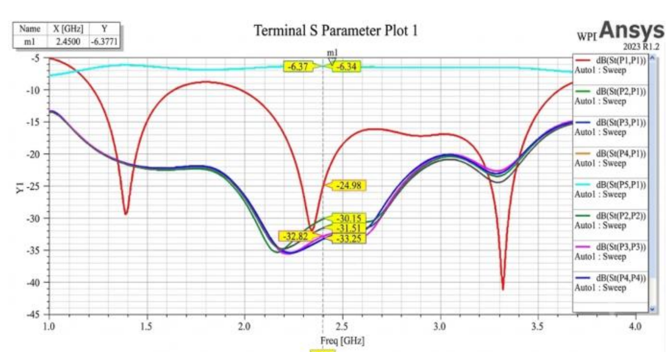

Fig. 15 S-parameter for Wilkinson power divider

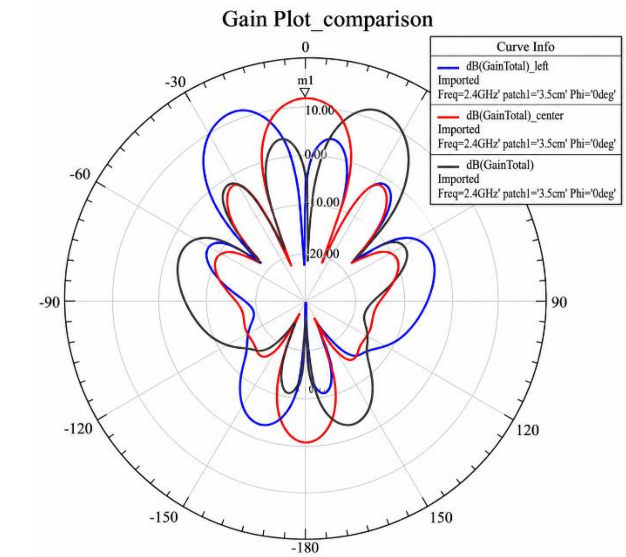

Fig. 16 Beam steering of patch array antenna

Table 4. Return loss at different beam steering angles at 2.45GHz

Beam Steering Angle	Return Loss
0º	13.7dB
-20º	22.51dB
20º	22.75dB

4.5. Thermal Analysis

The thermal response was calculated using the electromagnetic loss imported from HFSS. For an input power of 30 mW, the total EM loss was 0.007256 W. The maximum temperature obtained from the Icepak simulation was 20.019ºC, as shown in Figure 17. This small temperature rise suggests that the antenna array can operate safely at the investigated input power level. The simulation did not include additional heat sources from external circuits or biasing networks, so those effects should be considered in future hardware-level studies.

Compared with the related works summarized in Table 5, the proposed design is distinguished by the system-level integration of a MEMS-based DMTL phase-shifting network, four-way power divider, and four-element antenna array at 2.45 GHz. The integrated system achieves a maximum simulated gain of 10.56 dBi with beam steering from −20° to +20°. The use of MEMS-based DMTL phase shifters supports low-loss phase control, and the co-simulation workflow captures the interaction between the feed network, phase shifters, and antenna array. This integrated evaluation provides a clearer prediction of the system-level response than isolated component simulations.

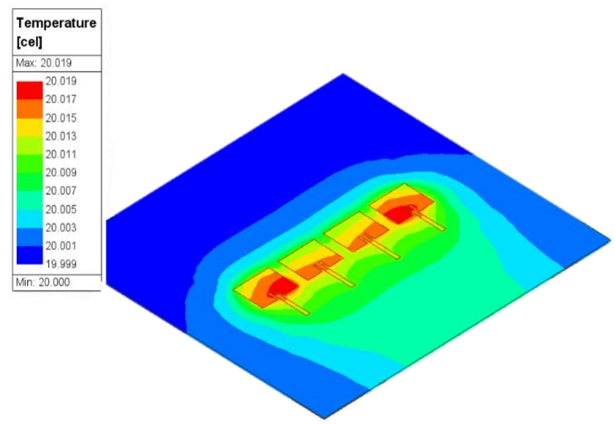

Fig. 17 Temperature distribution in ANSYS icepak

Table 5. Comparison with related phase-shifter and phased-array works

Work	Frequency	Phase Shifter Type	Gain	Beam Steering	Integration
[4]	25–50 GHz	5-bit PCM true-time-delay phase shifter, SiGe BiCMOS	N/A	N/A	Phase-shifter IC only
[5]	1.4 GHz	4-bit PIN-diode phase shifter	N/A	N/A	Phase shifter developed for an L-band radiometer antenna system
[6]	Dual-band	Filtering differential phase shifter	N/A	N/A	Component-level phase shifter
[7]	0-40 GHz	RF-MEMS DMTL phase shifter	N/A	N/A	Component-level phase shifter
[8]	18-40 GHz	RF-MEMS capacitive switch for DMTL	N/A	N/A	MEMS switch/component level
[9]	32GHz	3-state DMTL unit cell	N/A	N/A	Unit-cell/component level
[11]	15 GHz	3-bit RF-MEMS DMTL phase shifter	N/A	N/A	Phase-shifter level; intended for phased-array applications
This Work	2.45 GHz	MEMS-based DMTL phase shifter	10.56 dBi	−20° to +20°	Integrated phase shifter, power divider and 4-element array through co-simulation

5. Conclusion

This study demonstrated an integrated 2.45 GHz phased array antenna using MEMS-based DMTL phase-shifting elements. The DMTL phase shifter, Wilkinson power divider, and 4-element patch antenna array were first designed separately and then combined through ANSYS AEDT co-simulation. The completed system achieved beam steering from -20º to +20º with a maximum gain of 10.56 dBi. The DMTL phase shifter provided the required phase states with low insertion loss, while the Wilkinson divider supplied balanced power distribution to the antenna elements. Electrothermal simulation showed only a small temperature rise at 30 mW input power. Overall, the results demonstrate that the proposed co-simulation workflow can be used to evaluate RF, beam steering, and thermal behaviour of a compact MEMS-based phased array antenna system.

References

[1] Shuhao Shen, and Kang Zhou, "A Simple Dual-Band Coupler Design based on A Novel Dual-Mode Transmission Line Structure," *2024 IEEE MTT-S International Wireless Symposium (IWS)*, Beijing, China, pp. 1-3, 2024. [CrossRef] [Google Scholar] [Publisher Link]

[2] Low Ching Yu, and Muhammad Ramlee Kamarudin, "5G Fixed Beam Switching on Microstrip Patch Antenna," *International Journal of Electrical and Computer Engineering*, vol. 7, no. 2, pp. 975-980, 2017. [CrossRef] [Google Scholar] [Publisher Link]

[3] M. Kebe, M.C.E. Yagoub, and R.E. Amaya, "A Survey of Phase Shifters for Microwave Phased Array Systems," *International Journal of Circuit Theory and Applications*, vol. 53, no. 6, pp. 3719-3739, 2025. [CrossRef] [Google Scholar] [Publisher Link]

[4] Dimitrios Baltimas, and Gabriel M. Rebeiz, "A 25-50 GHz Phase Change Material (PCM) 5-Bit True Time Delay Phase Shifter in a Production SiGe BiCMOS Process," *2021 IEEE MTT-S International Microwave Symposium (IMS)*, Atlanta, GA, USA, pp. 435-437, 2021. [CrossRef] [Google Scholar] [Publisher Link]

[5] Kim Tuyen Trinh et al., "1.4 GHz Low-Cost PIN Diode Phase Shifter for ${L}$ -Band Radiometer Antenna," *IEEE Access*, vol. 7, pp. 95274-95284, 2019. [CrossRef] [Google Scholar] [Publisher Link]

[6] Lei-Lei Qiu, and Lei Zhu, "Dual-Band Filtering Differential Phase Shifter using Cascaded Wideband Phase Shifter and Bandstop Network with Two Same Phase Shifts," *IEEE Microwave and Wireless Components Letters*, vol. 31, no. 3, pp. 261-264, 2021. [CrossRef] [Google Scholar] [Publisher Link]

[7] V. Kumar, A. Basu, and S.K. Koul, "Low Actuation Voltage DMTL Phase Shifter with Improved Reliability," *2022 IEEE Microwaves, Antennas, and Propagation Conference (MAPCON)*, Bangalore, India, pp. 810-815, 2022. [CrossRef] [Google Scholar] [Publisher Link]

[8] G. Srihari, and T. Shanmuganantham, "Design and Analysis of MEMS based RF Capacitive Switch for DMTL Phase Shifter," *2019 TEQIP III Sponsored International Conference on Microwave Integrated Circuits, Photonics and Wireless Networks (IMICPW)*, Tiruchirappalli, India, pp. 154-158, 2019. [CrossRef] [Google Scholar] [Publisher Link]

[9] Mir Majid Teymoori, Seyyed Mehdi Mirebrahimi, and Massoud Dousti, "Design of a 3-State Unit Cell for DMTL Phase Shifters," *2021 Iranian International Conference on Microelectronics (IICM)*, Tehran, Iran, Islamic Republic of, pp. 1-4, 2021. [CrossRef] [Google Scholar] [Publisher Link]

[10] Ryan Ong, Salahuddin Raju, and M. Kumarasamy Raja, "Impact of Phase Shifter Design on Beam Squinting in Phased Array," *2021 IEEE International Symposium on Antennas and Propagation and USNC-URSI Radio Science Meeting (APS/URSI)*, Singapore, pp. 121-122. 2021. [CrossRef] [Google Scholar] [Publisher Link]

[11] N.M. Mary Sindhuja, and S. Kanthamani, "Three-Bit DMTL Phase Shifter for Phased Array Antennas," *Journal of Circuits, Systems and Computers*, vol. 28, no. 7, 2019. [CrossRef] [Google Scholar] [Publisher Link]

[12] Gabriel M. Rebeiz, *RF MEMS: Theory, Design, and Technology*, Wiley Online Library, pp. 1-18, 2003. [CrossRef] [Google Scholar] [Publisher Link]